

## Theoretical investigation of fundamental physical properties of full-Heusler $\text{Co}_2\text{VZ}$ ( $Z = \text{Al, Bi, Ga, Ge}$ ) compounds

S. Mahla<sup>a</sup>, R. Agrawal<sup>b</sup>, S. Kumar<sup>c</sup>, P. Singh<sup>d</sup>, M. Lal<sup>e</sup>, S. Singh<sup>f</sup>, A. S. Verma<sup>g,h,\*</sup>

<sup>a</sup>Department of Physics, GDC Memorial College, Bahal, Bhiwani 127028 India

<sup>b</sup>Department of Computer Engineering and Applications, G. L. A. University Mathura 281406 India

<sup>c</sup>Department of Physics, Dhanauri PG College, Roorkee, Haridwar 247667 India

<sup>d</sup>Department of Electronics and Communication Engineering, KIET Group of Institutions, Ghaziabad 201206, India

<sup>e</sup>Department of Physics, Government Degree College, Una, Himachal Pradesh 174303 India

<sup>f</sup>Department of Physics, Chintamani College of Arts and Science, Gondpipri, Maharashtra 442702 India

<sup>g</sup>Division of Research & Innovation, School of Applied and Life Sciences, Uttarakhand University, Dehradun, Uttarakhand 284007 India

<sup>h</sup>University Centre for Research & Development, Department of Physics, Chandigarh University, Mohali, Punjab 140413 India

A subclass of ternary intermetallic known as Heusler compounds is being employed in the steel industry to increase material strength. This study examines the structural, electrical, optical, and magnetic properties of  $\text{Co}_2\text{VZ}$  ( $Z = \text{Al, Bi, Ge, Si}$ ) compounds using two different methods. First is full potential linearized augmented plane wave (FP-LAPW) method by WIEN2k and second is pseudo potential method by Atomic Tool Kit-Virtual Nano-Lab. The equivalent energy gaps in the minority-spin of  $\text{Co}_2\text{VZ}$  ( $Z = \text{Al, Bi, Ga, Ge}$ ) with WIEN2k code, which displays 100% spin polarization, are 0.703, 0.384, 0.186, and 0.67 eV near to the Fermi level. Furthermore, it is discovered that these compounds are absolutely half-metallic ferromagnetic (HMF). With the exception of  $\text{Co}_2\text{VBi}$ , which exhibits metallic properties, the aforementioned compounds exhibit 0.525, 0.0, 0.553, and 0.786 eV band gaps in the ATK-VNL code and indicate 100% spin polarization. The magnetic moments of the compounds  $\text{Co}_2\text{VZ}$  ( $Z = \text{Al, Bi, Ga, Ge}$ ) are found to be 2.976, 4.003, 1.989, and 3.001  $\mu_B$ , respectively, in the WIEN2k code. The relative magnetic moments of the aforementioned compounds are also 1.991, 3.947, 1.999, and 2.997  $\mu_B$ , according to the ATK-VNL code.

(Received April 19, 2023; Accepted July 27, 2023)

**Keywords:** Heusler compounds, Half-metallic ferromagnetic, Band gap, Dielectric constant, Magnetic moment

### 1. Introduction

Full Heusler compounds have the L21 structure, which is made up of four interpenetrating FCC-lattices [1-3]. They are ternary compounds with the formula  $\text{X}_2\text{YZ}$  and the ratio 2:1:1. De Groot predicted the first Heusler alloys with half metallic ferromagnetism [4-6]. Half metallic Ferro-magnets (HMFs) exhibit 100% Fermi level spin polarization due to band structures that are metallic for the majority of spins and semiconducting for the minority spins. Half metallicity has received increased interest due to its numerous applications in Spintronics devices such as nonvolatile magnetic random-access memory, magnetic sensors, spin-resonant tunneling diodes, spintronic transistors, and spin light emitting diodes [7-14]. Felser et al. [15] have explained the spin-polarization of the p-like states of the N and O atoms is the fundamental source of half-metallicity in the  $\text{X}_2\text{RbCa}$  ( $X = \text{C, N, O}$ ) full-Heusler compounds. Bai et al. [16] have analysed the

\* Corresponding author: [ajay\\_phy@rediffmail.com](mailto:ajay_phy@rediffmail.com)  
<https://doi.org/10.15251/CL.2023.207.535>

Heusler family, focusing on the family's numerous applications in magnetic data storage, such as CPP-GMR read heads, MRAM arrays, and creating SPRAMs. These materials are ideal functional building blocks for spintronics devices. Sharma et al. [17] have observed that the  $\text{Fe}_2\text{CrAl}$  combination has a high density of states and is completely spin polarized around the Fermi level. Rai et al. [18] have also hypothesized that the Full-Heusler compound  $\text{Co}_2\text{CrGe}$  is a half-metallic ferrimagnetism utilizing the Generalized-gradient approximation for structural calculations and the local spin density approximation for electronic calculations. The  $\text{Co}_2\text{YZ}$  compounds were discovered to be half-metallic ferromagnetic, with an apparent linear relationship of the Curie temperature on the magnetic moment [19]. Co-based compounds were studied using ab initio methods among the Heusler compounds, and the majority of them were discovered to be HMFs [20-21]. Seema et al. [22] have studied the influence of disorder on the electrical, magnetic, and optical characteristics of  $\text{Co}_2\text{CrZ}$  ( $Z = \text{Al, Ga, Ge, Si}$ ) Heusler compounds using density functional theory. They investigate three types of disorders: DO3, A2, and B2, with the B2 disorder retaining spin polarisation and the DO3 and A2 disorders decreasing spin polarisation at the Fermi level. The structural, electronic, optical, and magnetic characteristics of  $\text{Co}_2\text{VZ}$  ( $Z = \text{Al, Bi, Ga, Ge}$ ) compounds were computed in this article utilising the WIEN2k code and the Atomistic Tool Kit-Virtual NanoLab (ATK-VNL) code under the Generalized-gradient approximation (GGA) for exchange correlation functions.

## 2. Theoretical analysis

For the fundamental physical characteristic's of  $\text{Co}_2\text{VZ}$  ( $Z = \text{Al, Bi, Ga, Ge}$ ) compounds, we have used Wien2k simulation package based on the density functional theory [23-25]. This is one of the most accurate methods for doing electronic structure computations on solids. The energy between core and valence states was adjusted at  $-6.0\text{Ry}$ . We have utilized 1000 k-points from the first Brillouin zone. For the calculation of optical properties, we used here 10000 k-points. The convergence or cutoff parameter  $R_{\text{mt}} K_{\text{max}}$  is set to 7.0, which is used to control the size of the basis sets. The radius of a plane wave is indicated by  $R_{\text{mt}}$ , while the maximum modulus of a reciprocal lattice vector is denoted by  $K_{\text{max}}$ . The energy convergence criteria was set at  $0.0001\text{Ry}$ . The maximum angular momentum ( $l_{\text{max}}$ ) value is assumed to be 10. The charge density and potential in the core area were calculated as a fourier series with a wave vector up to  $G_{\text{max}}=10$ . For the each atom muffin tin sphere radii ( $R_{\text{MT}}$ ) are tabulated in table 1.

Table 1. Muffin tin radius ( $R_{\text{MT}}$ ) for  $\text{Co}_2\text{VZ}$  ( $Z = \text{Al, Bi, Ga, Ge}$ ).

RMT (a.u.)	$\text{Co}_2\text{VAl}$	$\text{Co}_2\text{VBi}$	$\text{Co}_2\text{VGa}$	$\text{Co}_2\text{VGe}$
Co	2.33	2.38	2.33	2.34
V	2.21	2.38	2.22	2.22
Z	2.10	2.50	2.22	2.22

Herein, we have also used pseudo-potential technique in the framework of density functional theory, which was implemented in Atomistic Tool Kit-Virtual Nano-Lab (ATK-VNL) [26-27]. Using the Pulay Mixer technique, first-principles computations were used to explore the electrical and magnetic characteristics of  $\text{Co}_2\text{VZ}$  ( $Z = \text{Al, Bi, Ge, Si}$ ). We have utilized a double-zeta ( $\zeta$ ) polarized basis set for extending electron wave functions and GGA for studying exchange-correlation effects [24]. The atoms starting states for spin polarisation have been chosen as up and down. We employed  $10 \times 10 \times 10$  Monkhorst-Pack k-mesh [28] for brillouin zone sampling to maintain a balance between computational time and result accuracy. Furthermore, while optimising structures, we do not apply any constraints in the x, y, or z directions. The structures are allowed to be optimised until each atom achieves a force convergence criterion of  $0.05 \text{ eV}/\text{\AA}$ .

## 3. Results and discussions

### 3.1. Structural properties of Heusler compounds

The Full-Heusler compounds have a composition of 2:1:1 and a chemical formula of  $\text{X}_2\text{YZ}$ , with a structure of L21 (space group:  $225 \text{ Fm-3m}$ ) composed by four penetrating FCC-

lattices with atomic positions at X1 (1/4, 1/4, 1/4), X2 (3/4, 3/4, 3/4), Y (1/2, 1/2, 1/2), and Z (0, 0, 0). The atoms X and Y are transition metals, and the atom Z is a main group metal or semimetal. Murnaghan's [29] equation of state expresses the value of total energy and pressure as a function of volume as follows:

$$E(V) = E_0 + \left[ \frac{BV}{B_P} \left( \frac{1}{(B_P-1)} \left( \frac{V_0}{V} \right)^{B_P} + 1 \right) - \frac{BV_0}{(B_P-1)} \right]; \quad P(V) = \frac{B}{B_P} \left\{ \left( \frac{V_0}{V} \right)^{B_P} - 1 \right\}$$

$$\text{Pressure } (P) = -\frac{dE}{dV}, \quad B_P = -V \frac{dP}{dV} = V \frac{d^2E}{dV^2}$$

$E_0$  is the minimal energy at  $T = 0$  K,  $B$  is the bulk modulus,  $B_P$  is the pressure derivative of the bulk modulus, and  $V_0$  is the equilibrium volume in the preceding equations.

Figure 1 depicts the structure optimization findings. WIEN2k optimized lattice values for  $\text{Co}_2\text{VAl}$  and  $\text{Co}_2\text{VGe}$  are somewhat higher than ATK lattice parameters, whereas WIEN2k optimized lattice parameters for  $\text{Co}_2\text{VBi}$  and  $\text{Co}_2\text{VGa}$  are slightly lower than ATK-VNL optimized lattice parameters. Table 2 shows the calculated values of the optimized lattice parameter, equilibrium energy, and pressure derivative.

*Table 2. Lattice parameter, bulk modulus, equilibrium energy, and pressure derivative of  $\text{Co}_2\text{VZ}$  ( $Z = \text{Al, Bi, Ga, Ge}$ ).*

Compounds	Lattice parameter $a_0$ (Å)		Bulk modulus (GPa)		Equilibrium Energy (Ry)	Pressure derivative
	Calculated		Calculated			
	WIEN2k	ATK	WIEN2k	ATK		
$\text{Co}_2\text{VAl}$	5.751	5.794	211.59	172.96	-7958.307	3.482
$\text{Co}_2\text{VBi}$	6.178	6.099	156.56	198.36	-50635.487	3.663
$\text{Co}_2\text{VGa}$	5.772	5.676	196.61	216.10	-11360.840	4.108
$\text{Co}_2\text{VGe}$	5.776	5.794	266.24	215.75	-11670.772	
10.221						

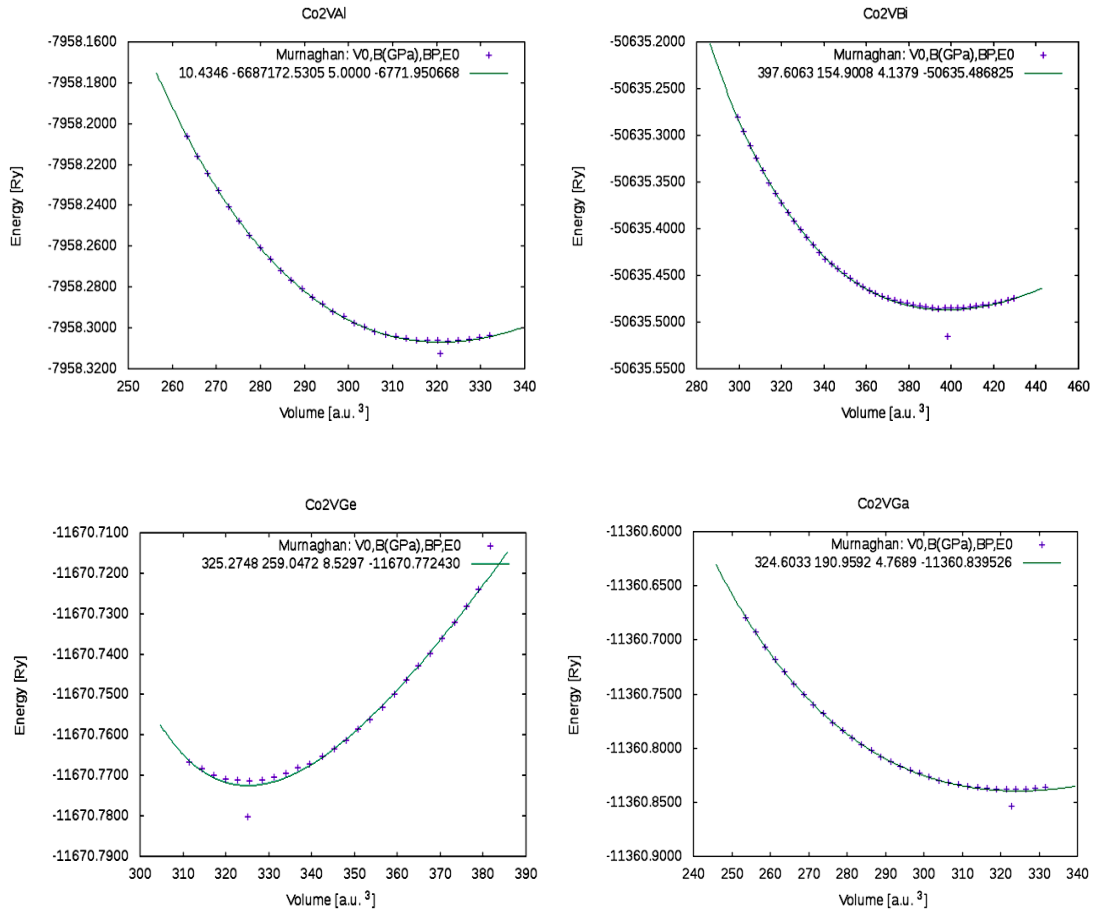


Fig. 1. Optimized lattice parameters.

### 3.2. Properties of electronic and magnetic Heusler compounds

At the optimized lattice parameters, spin polarized computations of  $\text{Co}_2\text{VZ}$  ( $Z = \text{Al, Bi, Ga, Ge}$ ) compounds were performed using the Generalized-gradient approximation (GGA) full Heusler. The computations indicated a gap in the minority states and zero gaps in the majority states at the Fermi level, resulting in 100% spin polarized band structure at the Fermi level. Magnetic moment is connected with spintronics owing to the inherent spin of the electron. The spin polarization has been determined theoretically using the provided formula.

$$P_n = \frac{n_{\uparrow} - n_{\downarrow}}{n_{\uparrow} + n_{\downarrow}}$$

If  $n_{\uparrow} = 0$  or  $n_{\downarrow} = 0$ ;  $P_n = 1$  or  $-1$ , only up or down spins occur, and spin polarization is 100%. These materials are known as half metal ferromagnetic or Heusler alloys with 100% spin polarization. If the value of  $P_n$  disappears, the materials are paramagnetic or anti-ferromagnetic even below the magnetic transition temperature [30]. This outstanding group of materials has a tremendous potential for many applications such as spintronics, magneto-electronic devices to boost data processing speed and integration density, and so on. The magnetic moment in Heusler alloy is a significant point in spintronics and follows the Slater-Pauling rule. This rule connects the magnetic moment per atom of transition element alloys to the average amount of valence electrons per atom:

$$m = N_v - 2N_{\downarrow}$$

where  $m$  represents the magnetic moment per atom in B,  $N_v$  represents the average number of valence electrons per atom, and  $N$  ( $N$ ) represents the number of minority spin (majority spin) valence electrons per atom. Non-volatility in materials is created by the component of spin degree of freedom [31]. Table 3 summarizes the obtained energy gap and spin polarization for the above approach. Figures 2-5 show the full results of band structures and density of states.

Table 3. Energy gap and spin polarization.

Compound	Energy gap $E_g$ (eV)				Spin polarization	
	WIEN2k		ATK		WIEN2k	ATK
	Up spin	Down spin	Up spin	Down spin		
$\text{Co}_2\text{VAl}$ 100%	0.0	0.703	0.0	0.525	100%	
$\text{Co}_2\text{VBi}$ vanishing	0.0	0.384	0.0	0.000	100%	$P_n$
$\text{Co}_2\text{VGa}$	0.0	0.186	0.0	0.553	100%	100%
$\text{Co}_2\text{VGe}$	0.0	0.670	0.0	0.786	100%	100%

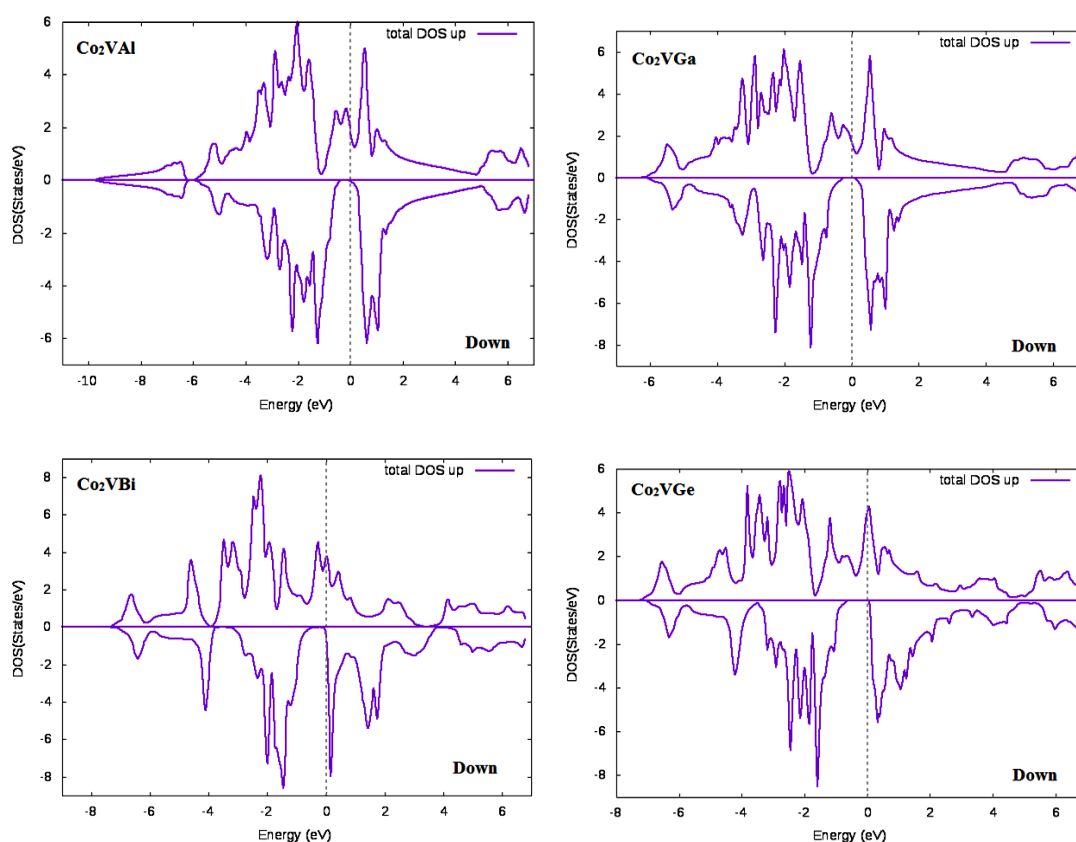


Fig. 2. DOS of  $\text{Co}_2\text{VZ}$  ( $Z = \text{Al}, \text{Bi}, \text{Ga}, \text{Ge}$ ) using WIEN2K Code.

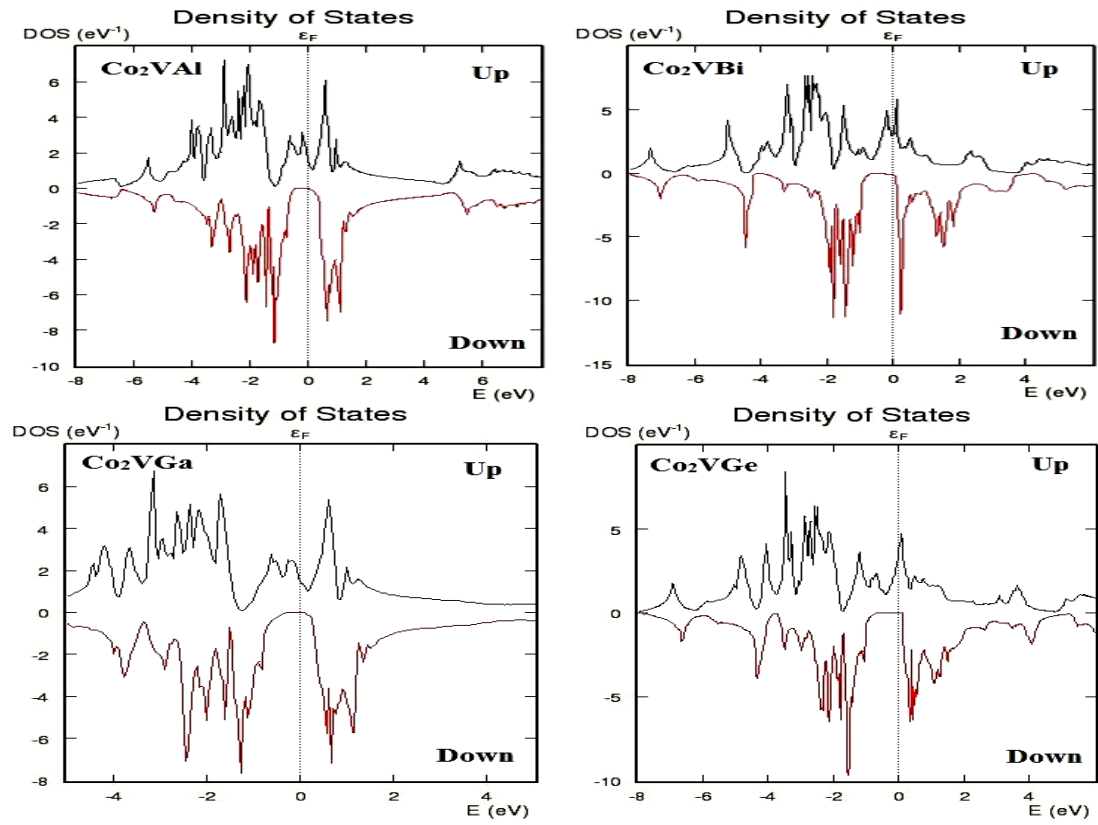


Fig. 3. DOS of  $\text{Co}_2\text{VZ}$  ( $Z = \text{Al}, \text{Bi}, \text{Ga}, \text{Ge}$ ) using ATK-VNL Code.



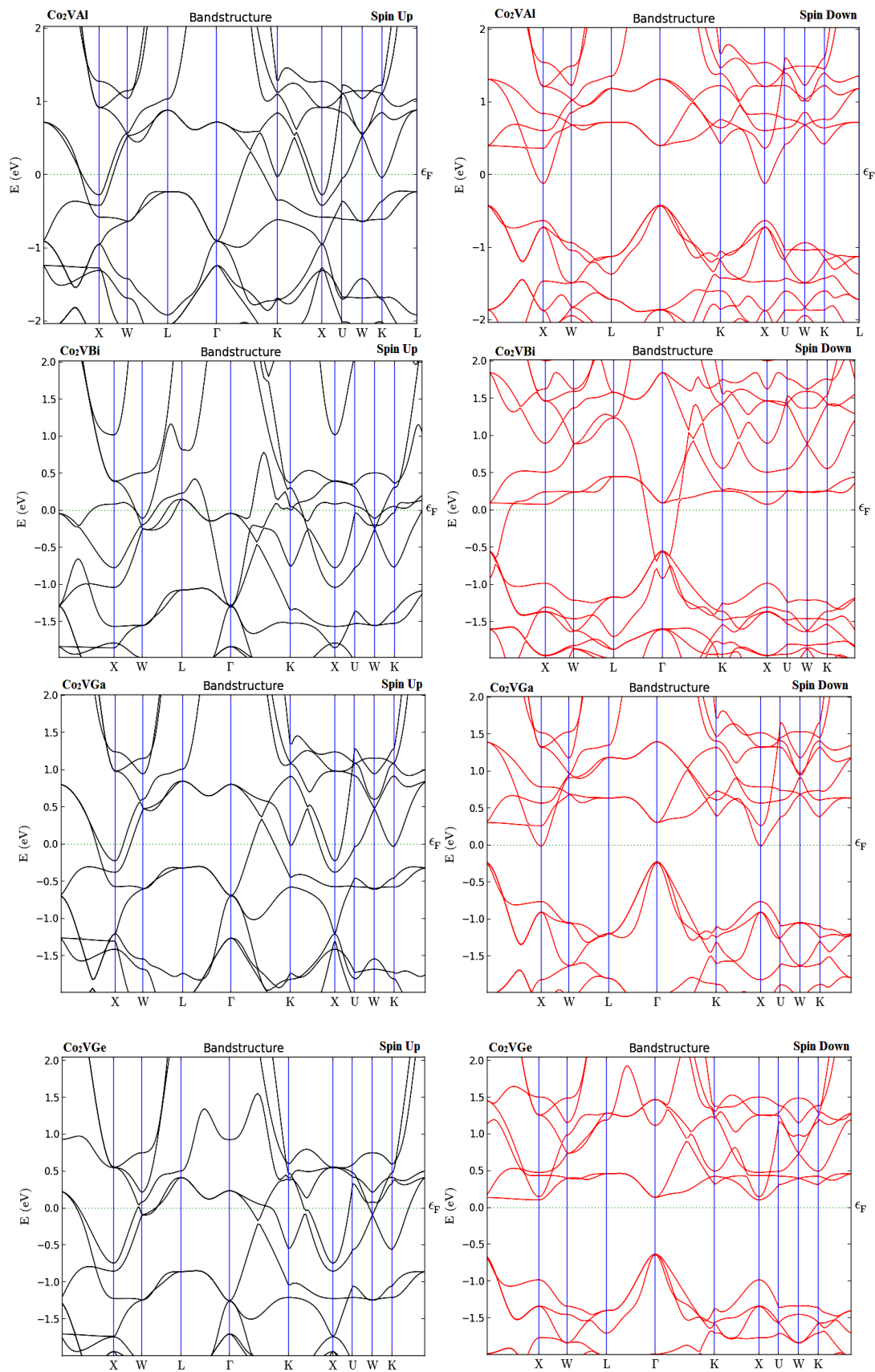


Fig. 5. Band structure of  $\text{Co}_2\text{VZ}$  ( $Z = \text{Al}, \text{Bi}, \text{Ga}, \text{Ge}$ ) using ATK-VNL Code.



The magnetic characteristics of Heusler alloys may be predicted by counting the number of valence electrons. With three transition metals per formula unit, 24 valence electron concentration semiconductors are feasible. For example, Fe<sub>2</sub>Val is a nonmagnetic semiconductor containing nonmagnetic iron. Co<sub>2</sub>YZ Heusler compounds contain more than 24 valence electron concentrations and obey the Slater-Pauling rule. If the number of valence electrons differs from 24, the magnetic moment per formula unit is exactly linked to the number of valence electrons minus 24 ( $M = Z_t - 24$ ). In this equation, M represents the total magnetic moment per unit cell, and  $Z_t$  represents the total amount of valence electrons. The complete Heusler compounds contain two separate magnetic sub-lattices, as opposed to the half Heusler compounds [21]. The Curie temperature of ferromagnetic half-metallic Heusler compounds increases by 175 K per additional electron. Co<sub>2</sub>CrAl, for example, contains 27 valence electrons with a saturation magnetization of 3 B/formula unit, is ferromagnetic with a magnetic moment that is mostly located on the Co sites, and has a Curie temperature of 525 K [15]. According to the findings, the magnetic moment resides mostly on the Co and Cr locations, whereas the Z position atom has a negligible tiny magnetic moment. It was discovered that Z atoms with more valence electrons had higher magnetic moments on both Co and Cr. The results also demonstrated that replacing Al with Si, Ge, or Bi enhances the localized magnetic moments on both sites at Co and Cr due to the addition of additional valence electrons. Localized magnetic moments rise at the X and Y sites when electronegativity increases. There is broad agreement on the Slater-Pauling behaviour. Here, we have found a very little difference between the FP-LAPW approach implemented in WIEN-2k and the pseudo-potentials method used in ATK-VNL. There is also considerable agreement amongst the approaches mentioned above and results are presented in Table 4.

### 3.3. Optical properties

Optical characteristics are vital in determining whether a material may be employed as an optoelectronics device. In this part, we will look at the optical characteristics of the compounds Co<sub>2</sub>VZ (Z= Al, Bi, Ga, Ge). For the optical characteristics, we compute the dielectric function, optical conductivity, reflectivity, excitation coefficient, absorption coefficient, and electron energy loss as a function of photon energy for the compounds. The optical response of a substance to incoming electromagnetic radiation is described by the complex dielectric function.

$$\varepsilon(\omega) = \varepsilon_1(\omega) + i\varepsilon_2(\omega)$$

where  $\varepsilon_1(\omega)$  represents the polarization and anomalous dispersion of the medium and  $\varepsilon_2(\omega)$  reflects the absorption or loss of energy into the medium [32- 33]. Figure 6 depicts the various optical spectra.

Table 4. Magnetic moments of Co<sub>2</sub>VZ (Z= Al, Bi, Ga, Ge) compounds.

Compound	$Z_t$  ( $Z_t - 24$ )	Magnetic moment ( $\mu_B$ )		
		WIEN2k	ATK	Slater-Pauling
Co <sub>2</sub> VAl	26	2.98	1.99	2.00
Co <sub>2</sub> VBi	28	4.00	3.95	4.00
Co <sub>2</sub> VGa	26	1.99	2.00	2.00
Co <sub>2</sub> VGe	27	3.00	3.00	3.00

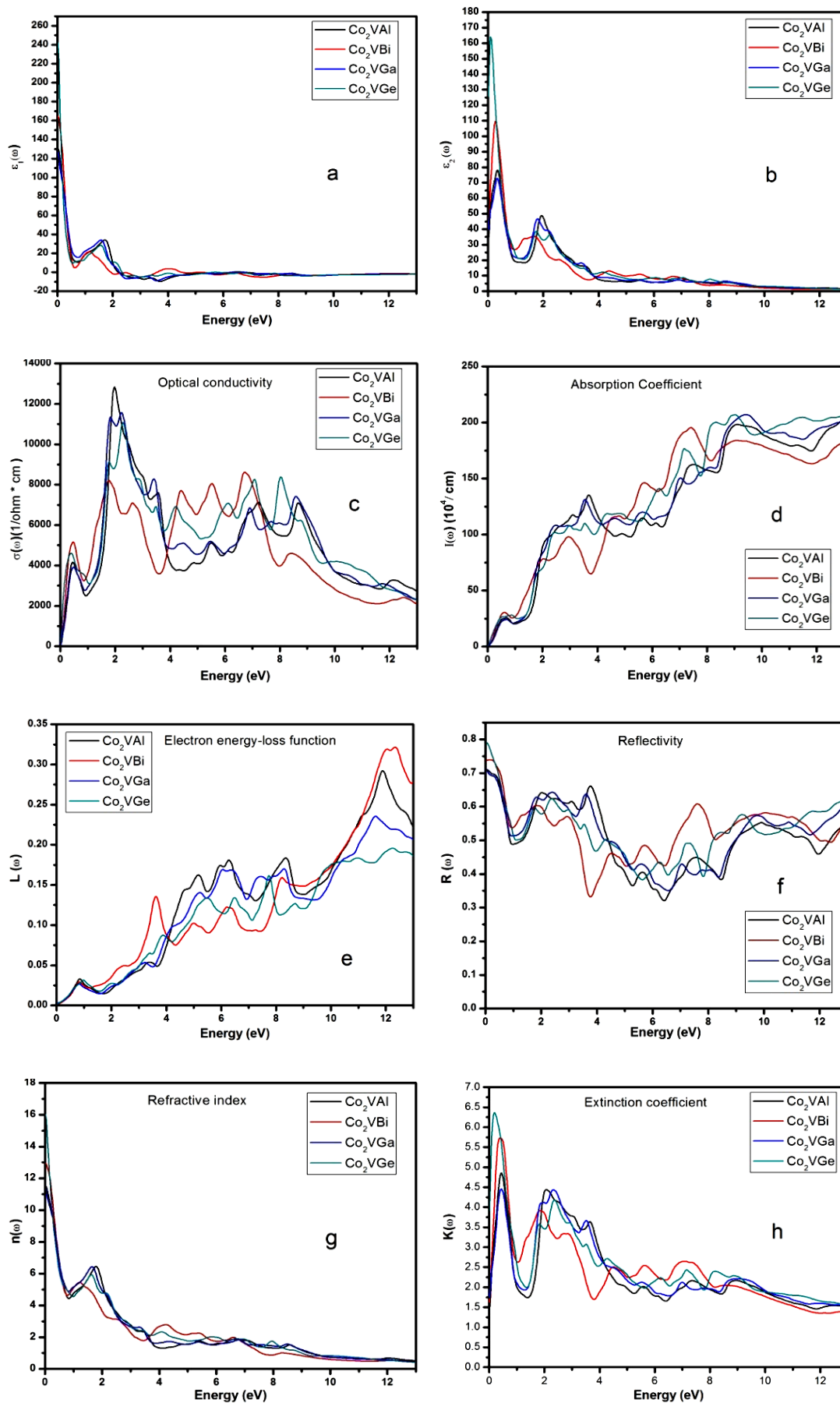


Fig. 6. Peaks of different optical spectra of these compounds.

For these compounds, imaginary dielectric function shows main peak in the visible region and after that decreases continuously as shown in figure 6 (b). Real and imaginary dielectric functions values are 130.803 and 32.470, 164.783 and 42.115, 126.797 and 39.608, 242.092 and 125.510 for  $\text{Co}_2\text{VZ}$  ( $Z = \text{Al, Bi, Ga, Ge}$ ) respectively presented in figures 6 (a) and 6 (b). An essential optical characteristic for electron conduction caused by an applied electromagnetic field is optical conductivity. A prominent peak is seen at 2 eV, and there are multiple peaks in the optical conductivity spectrum between 4.2 and 8.6 eV. Due to the material's high absorption coefficient, more photons that excite electrons from the valence band to the conduction band are absorbed by the material. As seen in figure 6(d), the values of the absorption coefficient rise as the energy values increase from the visible to the UV regions. The electron energy-loss function calculates the energy lost by an electron travelling quickly through a material. The frequency associated with plasma resonance and its strong peaks is known as the plasma frequency. When the frequency is higher than the plasma frequency, the material behaves as though it were dielectric, and when it is lower, it behaves as though it were metallic. As indicated in figure 6 (e) for the compounds above, the largest energy loss is seen between 11 and 13 eV, and the displacement of the extinction coefficient spectrum is displayed in figure 6 (h) above. In the visible spectrum, there is a noticeable peak, and in the UV spectrum, the value of the extinction coefficient diminishes. According to figure 6(f), the values of zero frequency reflectivity for the compounds  $\text{Co}_2\text{VZ}$  ( $Z = \text{Al, Bi, Ga, and Ge}$ ) are, respectively, 0.710, 0.737, 0.709, and 0.790. It is clear from the relationship between the absorption and reflection spectra that if absorption is highest, reflectivity must be minimal. The area when a substance significantly absorbs light and cannot reflect light efficiently within the same range. Because it affects things like the dispersive power of prisms, the focusing power of lenses, light guiding, and the critical angle for complete internal reflection, among other things, the refractive index is a crucial optical characteristic with many uses. The refractive index tells us how quickly light moves through the materials. The measured values for the compounds  $\text{Co}_2\text{VZ}$  ( $Z = \text{Al, Bi, Ga, Ge}$ ) for zero frequency refractive index are 11.532, 12.939, 11.394, and 16.043, respectively.

#### 4. Conclusions

In this work, we have investigated fundamental physical properties like as structural, electronic, optical and magnetic parameters of  $\text{Co}_2\text{VZ}$  ( $Z = \text{Al, Bi, Ga, and Ge}$ ) full-Heusler compounds by using two different theoretical simulation code WIEN-2k and ATK-VNL. The equivalent energy gaps in the minority-spin of  $\text{Co}_2\text{VZ}$  ( $Z = \text{Al, Bi, Ga, Ge}$ ) with WIEN2k code, which displays 100% spin polarization, are 0.703, 0.384, 0.186, and 0.67 eV near to the Fermi level.

With the exception of  $\text{Co}_2\text{VBi}$ , which exhibits metallic properties, the aforementioned compounds exhibit 0.525, 0.0, 0.553, and 0.786 eV band gaps in the ATK-VNL code and indicate 100% spin polarization. The magnetic moments of the compounds  $\text{Co}_2\text{VZ}$  ( $Z = \text{Al, Bi, Ga, Ge}$ ) have been found to be 2.976, 4.003, 1.989, and 3.001  $\mu_B$ , respectively by the WIEN2k code. The relative magnetic moments of the aforementioned compounds are also 1.991, 3.947, 1.999, and 2.997  $\mu_B$ , according to the ATK-VNL code. We have also studied their optical spectra for applications in spintronics and researchers may use expected findings in future studies.

#### References

- [1] Fr. Heusler and E. Take, *Trans. Faraday Soc.* 8, 169-184 (1912); <https://doi.org/10.1039/tf9120800169>
- [2] J. Li, Y. Li, G. Zhou, Y. Sun, and C. Q. Sun, *Appl. Phys. Lett.* 94, 242502 (2009); <https://doi.org/10.1063/1.3156811>
- [3] F. Casper, T. Graf, S. Chadov, B. Balke and C. Felser, *Semicond. Sci. Technol.* 27, 063001 (2012); <https://doi.org/10.1088/0268-1242/27/6/063001>

- [4] R. A. De Groot, F.M. Muller, P. G. Van Engen and K. H. J. Buschow, *Phys. Rev. Lett.* 50, 2024-2027 (1983); <https://doi.org/10.1103/PhysRevLett.50.2024>
- [5] Sukhender, L. Mohan, S. Kumar, D. Sharma, A. S. Verma, *East Eur. J. Phys.* 2, 69 (2020).
- [6] Sukhender, Pravesh, L. Mohan, A. S. Verma, *East Eur. J. Phys.* 3, 99-110 (2020).
- [7] Sukhender, Pravesh, L. Mohan, A. S. Verma, *East Eur. J. Phys.* 3, 111-121 (2020).
- [8] Sukhender, L. Mohan, A. S. Verma, *East Eur. J. Phys.* 4 51-62 (2020).
- [9] S. A. Khandy, I. Islam, D. C. Gupta and A. Lare, *J. Solid State Chem.* 270, 173-179 (2019); <https://doi.org/10.1016/j.jssc.2018.11.011>
- [10] T. Graf, C. Felser and S. S.P. Parkin, *Prog. Solid State Chem.* 39, 1-50 (2011); <https://doi.org/10.1016/j.progsolidstchem.2011.02.001>
- [11] M. Zipporah, P. Rohit, M. Robinson, M. Julius, S. Ralph, and K. Arti, *AIP Advances* 7, 055705 (2017); <https://doi.org/10.1063/1.4973763>
- [12] J. Kubler, G. H. Fecher, and C. Felser, *Phys. Rev. B* 76, 024414 (2007); <https://doi.org/10.1103/PhysRevB.76.024414>
- [13] Z. Q. Bai, Y. H. Lu, L. Shen, V. Ko, G. C. Han, and Y. P. Feng, *J. Appl. Phys.* 111, 093911 (2012); <https://doi.org/10.1063/1.4712301>
- [14] V. Ko, G. Han, J. Qiu, and Y. P. Feng, *Appl. Phys. Lett.* 95, 202502 (2009); <https://doi.org/10.1063/1.3263952>
- [15] C. Felser, L. Wollmann, S. Chadov, G. H. Fecher, and S. S. P. Parkin, *APL Mater.* 3, 041518 (2015); <https://doi.org/10.1063/1.4917387>
- [16] Z. Bai, L. Shen, G. Han and Y. P. Feng, *Spin* 2, 1230006 (2013); <https://doi.org/10.1142/S201032471230006X>
- [17] V. Sharma and G. Pilania, *J. Magn. Magn. Mater.* 339, 142150 (2013).
- [18] D. P. Rai, A. Shankar, Sandeep, M. P. Ghimire and R. K. Thapa, *J. Theor. Appl. Phys.* 7, 1-6 (2013); <https://doi.org/10.1186/2251-7235-7-3>
- [19] G. H. Fecher, H. C. Kandpal, S. Wurmehl, and C. Felser, *J. Appl. Phys.* 99, 08J106 (2006); <https://doi.org/10.1063/1.2167629>
- [20] M. Tas, E. Sasioglu, C. Friedrich, S. Blugel and I. Galanakis, *J. Appl. Phys.* 121, 053903 (2017); <https://doi.org/10.1063/1.4975351>
- [21] H. C Kandpal, G. H Fecher and C. Felser, *J. Phys. D* 40, 1587-1592 (2007); <https://doi.org/10.1088/0022-3727/40/6/S13>
- [22] K. Seema, N. M. Umran and R. Kumar, *J. Supercond. Nov. Magn.* 29, 401-408 (2016); <https://doi.org/10.1007/s10948-015-3271-7>
- [23] P. Blaha, K. Schwarz, G. K. H. Madsen, D. Kvasnicka and J. Luitz in *WIEN2k, An Augmented Plane Wave + Local Orbitals Program for Calculating Crystal Properties*, edited by K Schwarz (Technical Universitatwien, Austria, (2001), ISBN 3-9501031-1-2.
- [24] J. P. Perdew, K. Burke and M. Ernzerhof, *Phys. Rev. Lett.* 77, 3865-3868 (1996); <https://doi.org/10.1103/PhysRevLett.77.3865>
- [25] E. Sjostedt, L. Nordstrom and D. J Singh, *Solid State commun.* 114, 15-20 (2000); [https://doi.org/10.1016/S0038-1098\(99\)00577-3](https://doi.org/10.1016/S0038-1098(99)00577-3)
- [26] Atomistix ToolKit-Virtual Nanolab (ATK-VNL), QuantumWise Simulator, Version. 2014.3 [Online]. Available: <http://quantumwise.com/>
- [27] Y. J. Lee, M. Brandbyge, J. Puska, J. Taylor, K. Stokbro and M. Nieminen, *Phys. Rev. B*, 69, 125409 (2004); <https://doi.org/10.1103/PhysRevB.69.125409>
- [28] H. J. Monkhorst, and J. D. Pack, *Phys. Rev. B* 13, 5188-5192 (1976); <https://doi.org/10.1103/PhysRevB.13.5188>
- [29] F. D. Murnaghan, *Proc. Natl. Acad. Sci. U. S. A.* 30, 244-247 (1944); <https://doi.org/10.1073/pnas.30.9.244>
- [30] D. P. Rai and R. K. Thapa, *J. Alloys Comp.* 542, 257-263 (2012); <https://doi.org/10.1016/j.jallcom.2012.07.059>
- [31] S. Wurmehl, G. H. Fecher, H. C. Kandpal, V. Ksenofontov, and C. Felser, *Appl. Phys. Lett.*

88, 032503 (2006); <https://doi.org/10.1063/1.2166205>

[32] R. Jain, N. lakshmi, V. K. Jain, V. Jain, A. R. Chandra and K. Venugopalan, J. Magn. Magn. Mater. 448, 278-286 (2018); <https://doi.org/10.1016/j.jmmm.2017.06.074>

[33] S. Sharma, A. S. Verma and V. K. Jindal, Materials Research Bulletin 53, 218-233 (2014); <https://doi.org/10.1016/j.materresbull.2014.02.021>